Journal of Physics: Conference Series

PAPER • OPEN ACCESS

Vortex Artificial Potential Field for Mobile Robot Path Planning

To cite this article: A Nasuha *et al* 2022 *J. Phys.: Conf. Ser.* **2406** 012001

Vortex Artificial Potential Field for Mobile Robot Path Planning

A Nasuha, A S Priambodo, G N P Pratama

Department of Electronics and Informatics Engineering Education,
Universitas Negeri Yogyakarta, Indonesia.

E-mail: `arisnasuha@uny.ac.id`

Abstract. Artificial Potential Field (APF) is one of path planning strategies which offers a relatively low cost on computational. It has been implemented in many real-time applications. Unfortunately, it is quite susceptible to local minima problems. In this paper, we offer a scheme for escaping local minima by using vortex field. Based on the results and simulation, it can be verified that the vortex field prevails to navigate the path while escaping local minima.

1. Introduction

Today, autonomous robots can be found in many applications, such as military purposes, industries, even our daily lives [1]. Over the year, it gains more interest among researchers. There are various topics of research in robotics, and one of them is path planning. Path planning provides a solution for determining the path that should be taken by a robot for reaching the goal from its initial position [2]. There are many path planning strategies for mobile robot, such as Dijkstra [3], artificial potential field (APF) [4], rapidly exploring random tree (RRT) [5], A-star [6], and many more. Nevertheless, APF offers a relatively low computational complexity. Hence, it can be implemented in real-time scenario with ease. Historically, APF is introduced by Khatib in 1985 [7]. It consists of two virtual forces, namely attractive and repulsive force. The attractive force is designated at the goal that will attract the mobile robot. On the contrary, the repulsive forces are assigned to the obstacles that will move away the mobile robot. Those forces will drive the mobile robot toward the goal while avoiding the obstacles on its way [8].

Despite its simplicity, the conventional APF has some drawbacks. One of them is that the conventional APF is prone to local minima. It takes place when the total force is equal to zero. It may lead to such a condition that the mobile robot unable to move due to being trapped in local minima [9]. Previously, there are researches that have been conducted to tackle it. Some notable researches are conducted by Rizqi *et al.* [10] and Triharminto *et al.* [11], where they modify the repulsive field for escaping the local minima. Basically, by modifying the repulsive field, they also need to redefine the repulsive force [12, 13]. It requires such a thorough analysis.

Instead of modifying the repulsive field, the use of vortex field is proposed in this paper. It does not require us to modify the repulsive filed, we only need to define a new virtual force for the vortex field. It comes to handy since we can solve the problem with a simpler approach.

2. Artificial Potential Field

As mentioned before, that there are two main forces, here we discuss the attractive and repulsive force. We design the potential fields in $\mathbf{C} \in \mathbb{R}^2$, so we can drive the mobile robot toward the goal while avoiding any obstacles. The obstacles are occupying regions on $\mathbf{C_o}_i \in \mathbb{R}^2$.

2.1. Attractive Force

The attractive force should draw the mobile robot from its initial position to the goal. In order to do so, let us define the position of mobile robot as $\mathbf{q} = \begin{bmatrix} x & y \end{bmatrix}^{\mathrm{T}}$ meanwhile the goal be $\mathbf{q_g} = \begin{bmatrix} x_g & y_g \end{bmatrix}^{\mathrm{T}}$. Hence, the attractive potential can be defined as

$$U_a(q) = \frac{1}{2}k_a(\mathbf{q} - \mathbf{q_g})^2, \tag{1}$$

where $k_a > 0$ is the attractive gain. Based on equation (1), it can be said the attractive potential field is in a paraboloidal as shown in Figure 1.

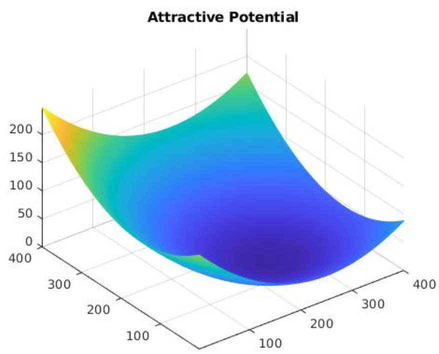

Figure 1. Attractive potential.

Next, we can determine the attractive force as gradient function of the attractive potential such as

$$\mathbf{F_a}(\mathbf{q}) = -\nabla U_a(\mathbf{q}). \tag{2}$$

2.2. Repulsive Force

The repulsive force is needed for avoiding the obstacles along the way. It will repel away the mobile robot. Let us define the repulsive potential as

$$U_r = \begin{cases} \frac{1}{2}k_r\left(\frac{1}{\rho} - \frac{1}{\rho_0}\right)^2 & , \text{ if } \rho \leq \rho_0, \\ 0 & , \text{ otherwise,} \end{cases} \tag{3}$$

where k_r and ρ_0 are the repulsive gain and the minimal distance between mobile robot and obstacle, that still affected by the repulsive potential. It should be noted that ρ_0 is given. Meanwhile, ρ is the distance between mobile robot and obstacle which can be denoted as

$$\rho = \sqrt{(\mathbf{q} - \mathbf{q_o})^2}, \tag{4}$$

$$\rho = \sqrt{(x - x_o)^2 + (y - y_o)^2}, \tag{5}$$

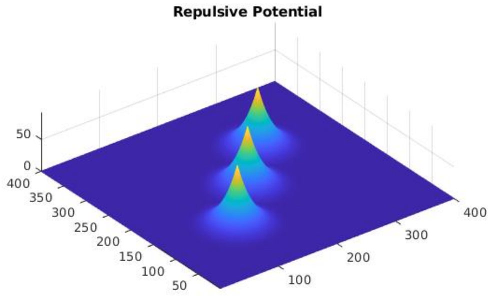

Figure 2. Repulsive potential.

where $\mathbf{q_o} = \begin{bmatrix} x_o & y_o \end{bmatrix}^{\mathrm{T}}$ is a vector position of the obstacle. If we have three obstacles at difference places, then the repulsive potential field can be depicted as shown in Figure 2.

Similarly as the attractive force, the repulsive force can be defined as the gradient function of repulsive potential, such as

$$\mathbf{F_r}(\mathbf{q}) = -\nabla U_r(\mathbf{q}). \tag{6}$$

2.3. Total Force

The total potential is sum of the attractive and repulsive potential, such as

$$U_t(\mathbf{q}) = U_a(\mathbf{q}) + U_r(\mathbf{q}). \tag{7}$$

Furthermore, if there are n number of obstacles, hence the total force can be denoted as

$$\mathbf{F_t}(\mathbf{q}) = -\nabla U_t(\mathbf{q}), \tag{8}$$

$$\mathbf{F_t}(\mathbf{q}) = \mathbf{F_a}(\mathbf{q}) + \sum_{i=1}^{n} \mathbf{F_{r_i}}(\mathbf{q}). \tag{9}$$

As an instance of the combined potential can be illustrated as in Figure 3.

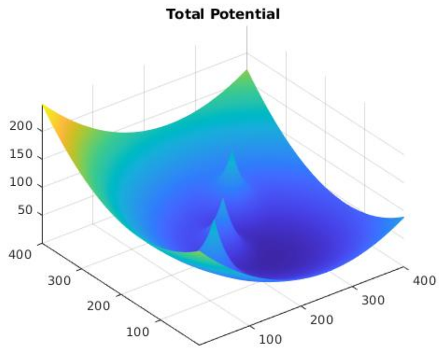

Figure 3. Total potential.

3. Local Minima and Vortex Field

In this section, the local minima problems and vortex field are discussed. Specifically, local minima due to SAROG (Symmetrically Aligned Robot-Obstacle-Goal) is explained in Subsection 3.1. Later, the solution by using vortex field is presented in Subsection 3.2.

3.1. Local Minima Problem

Generally, local minima problems are caused by repulsive force. Simply, by letting the attractive force is equal to the repulsive force, which implies that $\mathbf{F_t} = 0$, then the planned path will be stopped there. Ultimately, it is unable to reach the goal, even if there is a solution. Figure 4 depicts the condition of local minimum due to SAROG.

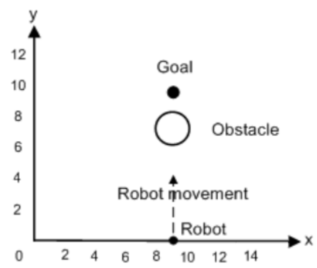

Figure 4. Goal in local minimum due to SAROG.

3.2. Vortex Field

We already knew that SAROG is caused by the repulsive actions near the obstacles. Here, instead of repelling the mobile robot, we can force it to move around the obstacle. Let us remind that $\mathbf{C} \in \mathbb{R}^2$, therefore we can denote the vortex field for $\mathbf{C_o}_i \in \mathbb{R}^2$ as

$$\mathbf{F_v} = \pm \begin{bmatrix} \frac{\partial U_{r_i}}{\partial y} \\ -\frac{\partial U_{r_i}}{\partial x} \end{bmatrix}. \tag{10}$$

It is expected that the intensity of the fields are still the same, the only changes are the directions. Apparently as long as $\mathbf{C_o}_i$ is convex, hence there is no local minima on the field. Figure 5 shows the vortex field direction, which can give a rough insight of how it works.

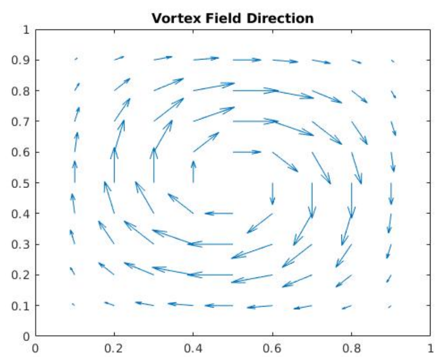

Figure 5. Vortex field direction.

4. Results and Analysis

There are two experiments that will be carried out by using MATLAB. First, the conventional APF is simulated under SAROG condition. It is necessary to verify that the conventional one is susceptible to local minima, hence it cannot reach the goal. Later, in the second experiment, we implement the vortex field for escaping the local minima.

Before any further, let us define the configuration space as follows. The initial position of mobile robot is at $\mathbf{q_s} = \begin{bmatrix} 50 & 350 \end{bmatrix}^\mathsf{T}$ and the goal is at $\mathbf{q_g} = \begin{bmatrix} 250 & 150 \end{bmatrix}^\mathsf{T}$. Meanwhile, there are three obstacles at $\mathbf{q_{o_1}} = \begin{bmatrix} 125 & 125 \end{bmatrix}^\mathsf{T}$, $\mathbf{q_{o_2}} = \begin{bmatrix} 200 & 200 \end{bmatrix}^\mathsf{T}$, and $\mathbf{q_{o_3}} = \begin{bmatrix} 275 & 275 \end{bmatrix}^\mathsf{T}$. The configuration space can be depicted as shown in Figure 6.

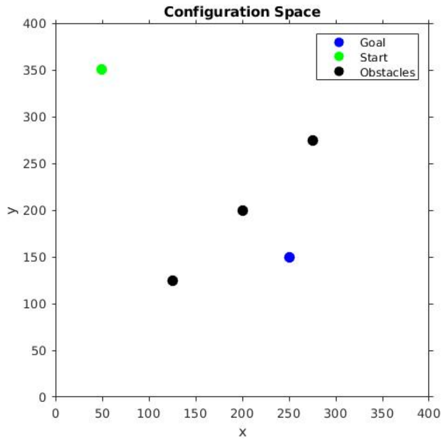

Figure 6. Configuration space.

The initial position of the mobile robot and the goal are represented by a green and blue circle. On the other hand, the obstacles are represented by the black circles. Clearly, we can see from Figure 6, that the initial position of mobile robot, obstacle number 2, and the goal are aligned to each others.

4.1. Conventional APF

It should be noted that in this simulation we need to determine the maximum number of iteration for computing the path. If the maximum number of iteration is not defined, there is a possibility that it will keep searching the path endlessly while being trapped in local minima. Here the maximum number of iteration is 1000. As long as the path to the goal can be found without exceeding the limit, then it is a success.

It just as we expected, when the problem arises, the path generated by the conventional APF cannot reach the goal as depicted in Figure 7.

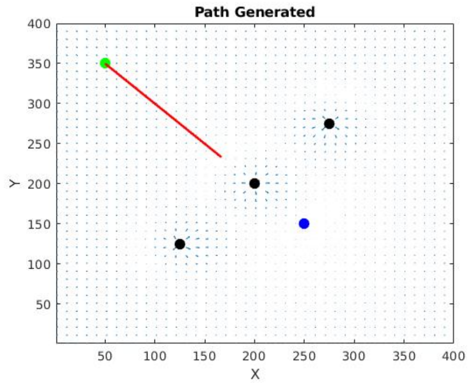

Figure 7. Path generated by conventional APF.

The generated path, the red line, is stopped near the obstacle number 2. It cannot move further neither step back, since it is trapped in local minimum. Eventually, it can be concluded that the conventional one is not suitable for this scenario, we need to employ a difference approach in order to overcome it.

4.2. APF with Vortex Field

Unlike the conventional one, after implementing vortex field, it succeeds reaching the goal as illustrated in Figure 8.

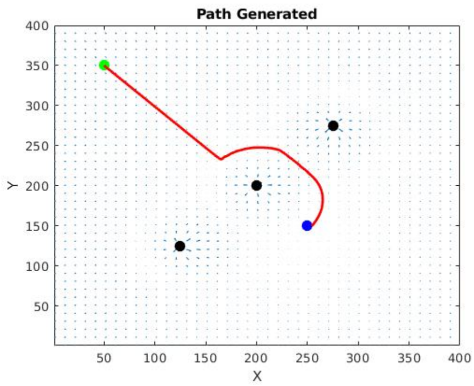

Figure 8. Path generated by APF with vortex field.

It can escape from local minima due to SAROG by moving around on the left direction, approaching the obstacle number 3. Basically, from equation (10), the vortex field direction can be assigned either clock-wise or counter-clock-wise, which depends on the signs. It implies that the path also can be directed to turn to the right, approaching the obstacle number 1.

5. Conclusion

In this paper, we present the implementation of vortex field for escaping the local minima due to SAROG. Here, we also simulate the conventional APF for comparison. It cannot escape the local minima and trapped near the obstacle. Meanwhile, our proposed scheme, by introducing vortex field, succeeds on leading the path to the goal. It verifies that the local minima due to SAROG can be tackled by using a vortex field, which is simpler than modifying the repulsive field like previous researches.

References

[1] A. R. Khan, A. T. Khan, M. Salik, and S. Bakhsh. An optimally configured hp-gru model using hyperband for the control of wall following robot. *International Journal of Robotics and Control Systems*, 1(1):66–74, 2021.

[2] Lasmadi, A. Cahyadi, S. Herdjunanto, and R. Hidayat. Inertial navigation for quadrotor using kalman filter with drift compensation. *International Journal of Electrical and Computer Engineering*, 7(5):2596–2604, 2017.

[3] E. W. Dijkstra. A note on two problems in connexion with graphs. *Numerische Mathematik*, 1(1):269–271, 1959.

[4] O. Khatib. Real-time obstacle avoidance for manipulators and mobile robots. *International Journal of Robotics Research*, 5(1):90–98, 1986.

[5] S. M. LaValle and J. J. Kuffner Jr. Randomized kinodynamic planning. *International Journal of Robotics Research*, 20(5):378–400, 2001.

[6] S. A. Gunawan, G. N. P. Pratama, A. I. Cahyadi, B. Winduratna, Y. C. H. Yuwono, and O. Wahyunggoro. Smoothed a-star algorithm for nonholonomic mobile robot path planning. In *2019 International Conference on Information and Communications Technology (ICOIACT)*, pages 654–658, 2019.

[7] O. Khatib. Real-time obstacle avoidance for manipulators and mobile robots. In *Proceedings. 1985 IEEE International Conference on Robotics and Automation*, volume 2, pages 500–505, 1985.

[8] K. Nakazawa, K. Takahashi, and M. Kaneko. Unified environment-adaptive control of accompanying robots using artificial potential field. In *2013 8th ACM/IEEE International Conference on Human-Robot Interaction (HRI)*, pages 199–200, 2013.

[9] M. H. Mabrouk. Crowd behavior simulation using artificial potential fields. *IAENG International Journal of Computer Science*, 40(4):220–229, 2013.

[10] A. A. A. Rizqi, A. I. Cahyadi, and T. B. Adji. Path planning and formation control via potential function for uav quadrotor. In *2014 International Conference on Advanced Robotics and Intelligent Systems (ARIS)*, pages 165–170, 2014.

[11] H. H. Triharminto, O. Wahyunggoro, T. B. Adji, and A. I. Cahyadi. An integrated artificial potential field path planning with kinematic control for nonholonomic mobile robot. *International Journal on Advanced Science, Engineering and Information Technology*, 6(4):410–418, 2016.

[12] H. H. Triharminto, O. Wahyunggoro, T. B. Adji, A. I. Cahyadi, and I. Ardiyanto. A novel of repulsive function on artificial potential field for robot path planning. *International Journal of Electrical and Computer Engineering*, 6(6):3262–3275, 2016.

[13] H. H. Triharminto, O. Wahyunggoro, T. B. Adji, A. Cahyadi, I. Ardiyanto, and Iswanto. Local information using stereo camera in artificial potential field based path planning. *IAENG International Journal of Computer Science*, 44(3):316–326, 2017.